CHEMISTRY OF MATERIALS
Article

Chem. Mater. **2010,** *22,* 2367–2374 2367
DOI:10.1021/cm9036633

Patterned Carbon Nanotubes with Adjustable Array: A Functional Breath Figure Approach

Chun-Yin Ma,[†] Ya-Wen Zhong,[‡] Jian Li,[‡] Cai-Kang Chen,[‡] Jian-Liang Gong,[‡] Su-Yuan Xie,*[,†] Lei Li,*[,‡] and Zhi Ma[§]

[†]*College of Chemistry and Chemical Engineering, and* [‡]*College of Materials, Xiamen University, Xiamen 361005, P. R. China, and* [§]*Shanghai Institute of Organic Chemistry, Chinese Academy of Sciences, Shanghai 200032, P. R. China*

Received December 4, 2009. Revised Manuscript Received February 4, 2010

Patterning is of paramount importance in many areas of modern science and technology. As a valuable part in miniaturized devices, large-scale aligned CNTs with serial port configuration is highly desirable. Here, we reported that the synthesis of a pair of patterned carbon nanotubes with the shape of serial port by CVD starting from different breath figure templates, cross-linked polymer matrix and ferrous inorganic micropatterns. The growth mechanism of the isolated CNT bundles is attributed to the selectively interfacial aggregation of the ferrocene to the walls of the cavities, a so-called Pickering-emulsion effect, whereas the honeycomblike skeleton of the dense CNT arrays develop from the catalytically functionalized hexagonal edges. This synthesis strategy exemplifies a new possibility for making use of CNTs to fabricate functional carbons with unique geometry or specific properties in a controllable way. We expect that the methodology can be also applied onto the fabrication of patterned graphene.

Patterning is of paramount importance in many areas of modern science and technology with applications ranging from the production of integrated circuits, information storage devices, and display units to the fabrication of microelectromechanical systems, miniaturized sensors, micro fluids devices, biochips, photonic bandgap crystals, micro-optical components, and diffractive optical elements.[1] Research on the synthesis of patterned carbon nanotubes (CNTs) with controllable location and orientation has attracted ever-increasing attention,[2] largely due to its technological importance for applications such as scanning probe microscopy,[3] supercapacitor,[4] and field-emission flat panel displays.[5] As a valuable part in miniaturized devices, large-scale aligned CNTs with serial port configuration is highly desirable.[6] The controllable CNT architectures have been achieved by chemical vapor deposition (CVD) on predesigned catalyst patterns or substrate patterns, constructed by a variety of strategies including offset printing, standard lithography, and soft lithography.[7] By means of the available techniques, the space resolution for the preparation of CNT patterns on substrate has been down to micrometer scale. However, the time and cost involved in generating the patterns are the major barriers to limiting the use of the available technologies such as lithography. In contrast, self-assembly provides efficient and fundamentally simple methods for creating microstructures. Breath figure (BF) process is one of the most promisingly self-assembling strategies for the fabrication of large size patterns having an ordered two-dimensional array of holes.[8] However, application of the BF method in CNT growth is still scarce. In this article, we describe the fabrication of a pair of patterned CNTs arrays with matchable serial port configuration by means of the ferrous microporous templates stemming from a static BF process.

In a typical BF process, polymer in a water-immiscible solvent is cast under high humidity. Hexagonally packed water microdroplets are formed by evaporation cooling

*To whom correspondence should be addressed. E-mail: lilei@xmu.edu.cn (L.L.); syxie@xmu.edu.cn (S.-Y.X.).

(1) Geissler, M.; Xia, Y. N. *Adv. Mater.* **2004**, *16*, 1249.
(2) (a) Fan, S. S.; Chapline, M. G.; Franklin, N. R.; Tombler, T. W.; Cassell, A. M.; Dai, H. J. *Science* **1999**, *283*, 512. (b) Wei, B. Q.; Vajtai, R.; Jung, Y.; Ward, J.; Zhang, R.; Ramanath, G.; Ajayan, P. M. *Nature* **2002**, *416*, 495. (c) Hata, K.; Futaba, D. N.; Mizuno, K.; Namai, T.; Yumura, M; Iijima, S. *Science* **2004**, *306*, 1362.
(3) Hafner, J. H.; Cheung, C. L.; Lieber, C. M. *Nature* **1999**, *398*, 761.
(4) Futaba, D. N.; Hata, K.; Yamada, T.; Hiraoka, T.; Hayamizu, Y.; Kakudate, Y.; Tanaike, O.; Hatori, H.; Yumura, M.; Iijima, S. *Nat. Mater.* **2006**, *5*, 987.
(5) Bonard, J.; Stöckli, T.; Noury, O.; Châtelain, A. *Appl. Phys. Lett.* **2001**, *78*, 2775.
(6) (a) Baughman, R. H.; Zakhidov, A. A.; de Heer, W. A. *Science* **2002**, *297*, 787. (b) Melechko, A. V.; Merkulov, V. I.; McKnight, T. E.; Guillorn, M. A.; Klein, K. L.; Lowndes, D. H.; Simpson, M. L. *J. Appl. Phys.* **2005**, *97*, 041301.
(7) (a) Bennett, R. D.; Hart, A. J.; Miller, A. C.; Hammond, P. T.; Irvine, D. J.; Cohen, R. E. *Langmuir* **2006**, *22*, 8273. (b) Teo, K. B. K.; Chhowalla, M.; Amaratunga, G. A. J.; Milne, W. I.; Legagneux, P.; Pirio, G.; Gangloff, L.; Pribat, D.; Semet, V.; Binh, V. T.; Bruenger, W. H.; Eichholz, J.; Hanssen, H.; Friedrich, D.; Lee, S. B.; Hasko, D. G.; Ahmed, H. *J. Vac. Sci. Technol. B* **2003**, *21*, 693. (c) Lastella, S.; Jung, Y. J.; Yang, H.; Vajtai, R.; Ajayan, P. M.; Ryu, C. Y.; Rider, D. A.; Manners, I. *J. Mater. Chem.* **2004**, *14*, 1791. (d) Vieira, S. M. C.; Teo, K. B. K.; Milne, W. I.; Gröning, O.; Gangloff, L.; Minoux, E.; Legagneux, P. *Appl. Phys. Lett.* **2006**, *89*, 022111.
(8) Widawski, G.; Rawieso, M.; François, B. *Nature* **1994**, *369*, 387.

Published on Web 02/16/2010

on the solution surface and then transferred to the solution front in the convectional flow or by the capillary force. After solvent evaporation, the honeycomb-patterned polymer film is formed with the water droplet array as a template. Finally, microporous polymer films are obtained after water evaporation. Various types of polymers can be fabricated as a honeycomb-patterned film with controlled pore size, ranging from hundreds of nanometers to hundreds of micrometers.[9] The simple method offers new prospects in the field of microporous films, as well as other technical advantages of low-cost and large area applicability. Quite recently, we developed a robust static BF process to fabricate ordered microstructured polymer films. Amphiphilic diblock copolymer polystyrene-*b*-poly(acrylic acid) (PSPAA), commercially available triblock copolymer polystyrene-*b*-polybutadiene-*b*-polystyrene (SBS), even linear PS without polar end groups and mixtures of PSPAA/inorganic precursors were found forming regularly microporous films in a wide solution concentration range tolerating temperatures, molecular weights, and chemical compositions.[10] Moreover, the microporous polymer matrix could be further modified by UV irradiation to serve as cell scaffolds or converted into inorganic micropatterns by pyrolysis to act as templates to create honeycomb structured inorganic arrays. Herein, the static BF processes are employed to synthesize a pair of matchable serial-port-shaped CNT patterns, i.e., the isolated CNT bundle arrays and the honeycomb-like skeleton with the walls of vertically dense CNT bundles, on Si wafer after CVD process. To circumvent the expensive lithographic technique, the reported methodology apparently provides a facile preparation of patterned CNT serial port that may be useful for engineering applications.

The fabrication process of serial-port-shaped aligned CNT bundles on substrate is schematically shown in Figure 1. First, a mixture of PSPAA/ferrocene (5/1, w/w) was dissolved in CS_2. Then the solution was casted on Si wafer by a microsyringe. After evaporation of solvent in saturated relative humidity, a highly regularly microstructured hybrid film was formed (Figure 1a). Followed by UV irradiation, the thermal stability of the polymer matrix was improved through cross-linked behavior, whereas the honeycomb structures were intact (Figure 1b). Such a cross-linked polymer matrix can act as the template for CVD growth of isolated CNT bundle arrays (Figure 1d), or serve as the structure-directing model for further pyrolysis to form ferrous inorganic micropatterns (Figure 1c) in which ferrocene was partially oxidized and replaced the skeleton of polymer matrix. The honeycomb-like skeleton with the walls of vertically dense CNT bundles

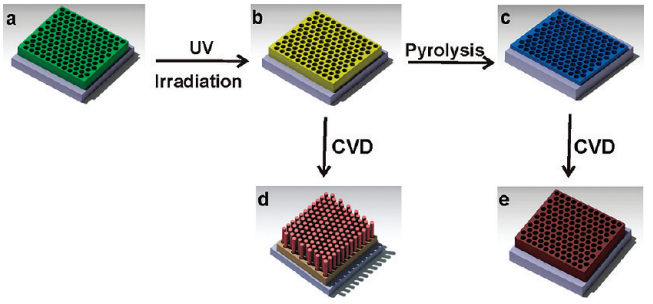

Figure 1. Schematic pictures of fabrication process of serial-port-shaped aligned CNT bundles on substrate. (a) Highly regular microstructured PSPAA/ferrocene hybrid film was formed on substrate after total evaporation of solvent under high humidity. (b) Polymer matrix was cross-linked and the honeycomb structures were preserved after photochemical process. (c) Ferrous inorganic micropatterns in honeycomb structures were formed on substrate after pyrolysis. (d) Isolated CNT bundles were developed templating from the cross-linked microporous polymer film. (e) Dense CNT bundles in hexagonal shape were formed under guidance by the inorganic micropatterns.

(i.e., another end of a pair of serial-port-shaped aligned CNT bundles) were synthesized guided by the inorganic micropatterns (Figure 1e).

As reported in our previous publications,[10] static BF process is a robust methodology to prepare ordered microporous polymer films, because any uncertainties caused by airflow disturbing are minimized. More variables are tolerated in casting conditions, including molecular weights, temperature, solution concentrations, different polymer architectures, and chemical compositions. Herein, the same static BF process as described in the Experimental Section is employed to prepare regular PSPAA/ferrocene hybrid films. Figure 2a is the photograph of silicon wafer, on which a structured PSPAA/ferrocene hybrid film has formed. As expected from the highly ordered structures, the film exhibits an interesting nacre color because of sunlight diffraction and interference effects.[11] More precise microscopy studies by scanning electronic microscopy (SEM) and atomic force microscopy (AFM) are shown in Figure 2b,c, respectively. It is clear that the film surface is made up by one layer of highly ordered honeycomb structures with identical size. The associated fast Fourier transform (FFT) of the SEM image (the inset in Figure 2b), with first- and high-order spots, demonstrates the very regular character of the main structures. Though a large amount of ferrocene is incorporated into polymer matrix, no macrophase separation is observed in the whole film area. For more detailed insight into the geometry, we show the considerably magnified AFM height image in Figure 2c. The AFM image gives the pore diameter and average pore separation as 1.3 and 3.5 μm, respectively, which are consistent with the SEM results. Either top or cross-sectional view (Figure 2d) reveals that the resultant film has a monolayer of independent pores on dense polymer stratum without network structures. Generally speaking, hybridization of organic polymer with inorganic structure may combine the merits of both components.

(9) (a) Bunz, U. H. F. *Adv. Mater.* **2006**, *18*, 973. (b) Stenzel, M. H.; Barner-Kowollik, C.; Davis, T. P. *J. Polym. Sci., Part A* **2006**, *44*, 2363.

(10) (a) Li, L.; Chen, C. K.; Zhang, A. J.; Liu, X. Y.; Cui, K.; Huang, J.; Ma, Z.; Han, Z. H. *J. Colloid Interface Sci.* **2009**, *331*, 446. (b) Li, L.; Chen, C. K.; Li, J.; Zhang, A. J.; Liu, X. Y.; Xu, B.; Gao, S. B.; Jin, G. H.; Ma, Z. *J. Mater. Chem.* **2009**, *19*, 2789. (c) Li, L.; Zhong, Y. W.; Li, J.; Chen, C. K.; Zhang, A. J.; Xu, J.; Ma, Z. *J. Mater. Chem.* **2009**, *19*, 7222. (d) Li, L.; Zhong, Y. W.; Ma, C. Y.; Li, J.; Chen, C. K.; Zhang, A. J.; Tang, D. L.; Xie, S. Y.; Ma, Z. *Chem. Mater.* **2009**, *21*, 4977.

(11) Billon, L.; Manguian, M.; Pellerin, V.; Joubert, M.; Eterradossi, O.; Garay, H. *Macromolecules* **2009**, *42*, 345.

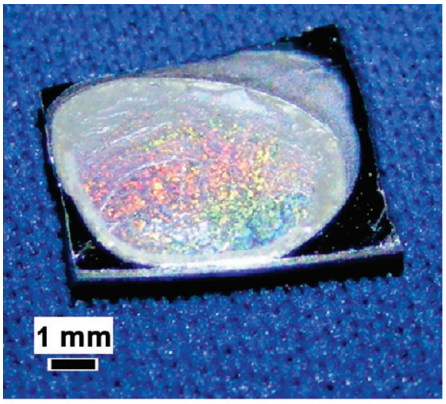

a

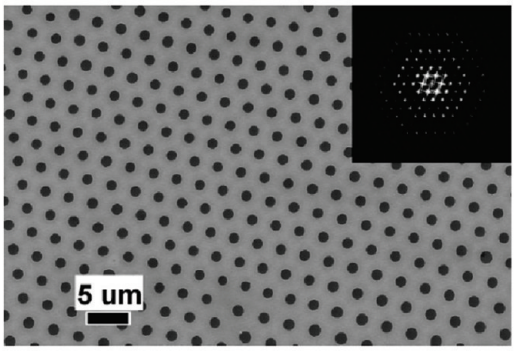

b

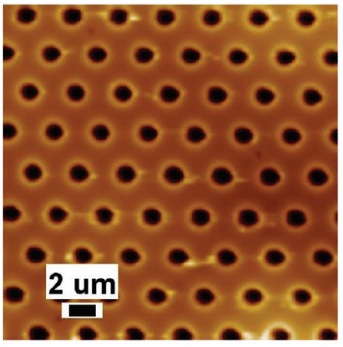

c

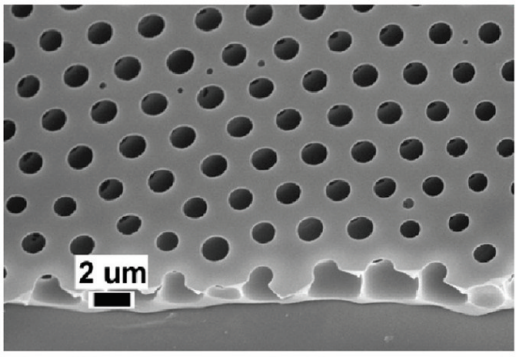

d

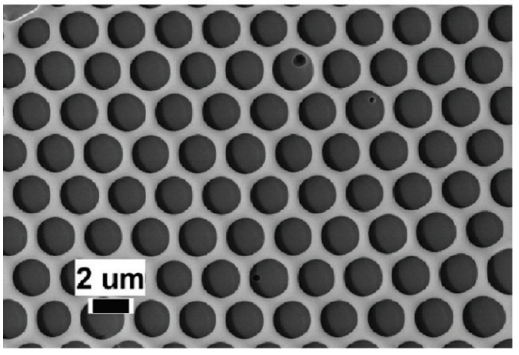

e

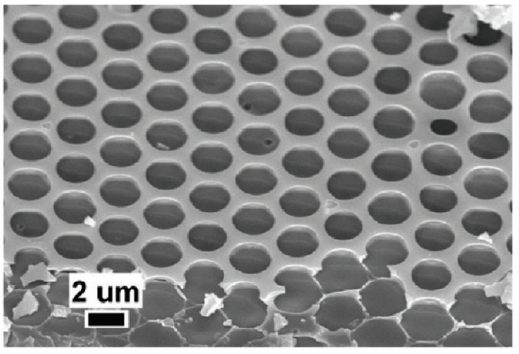

f

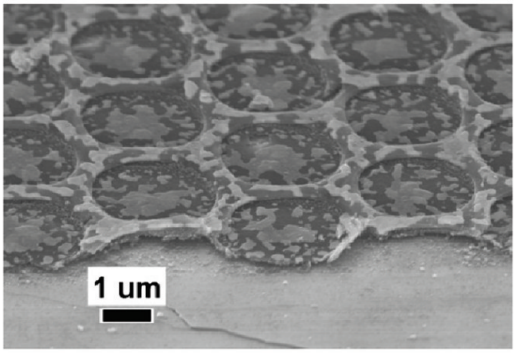

g

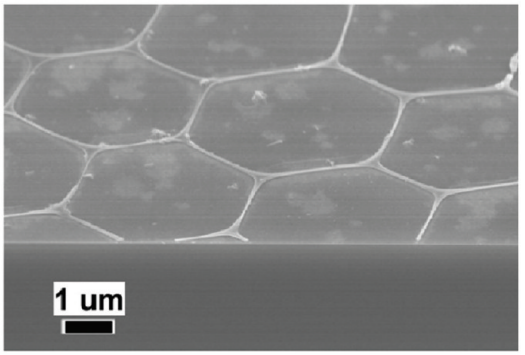

h

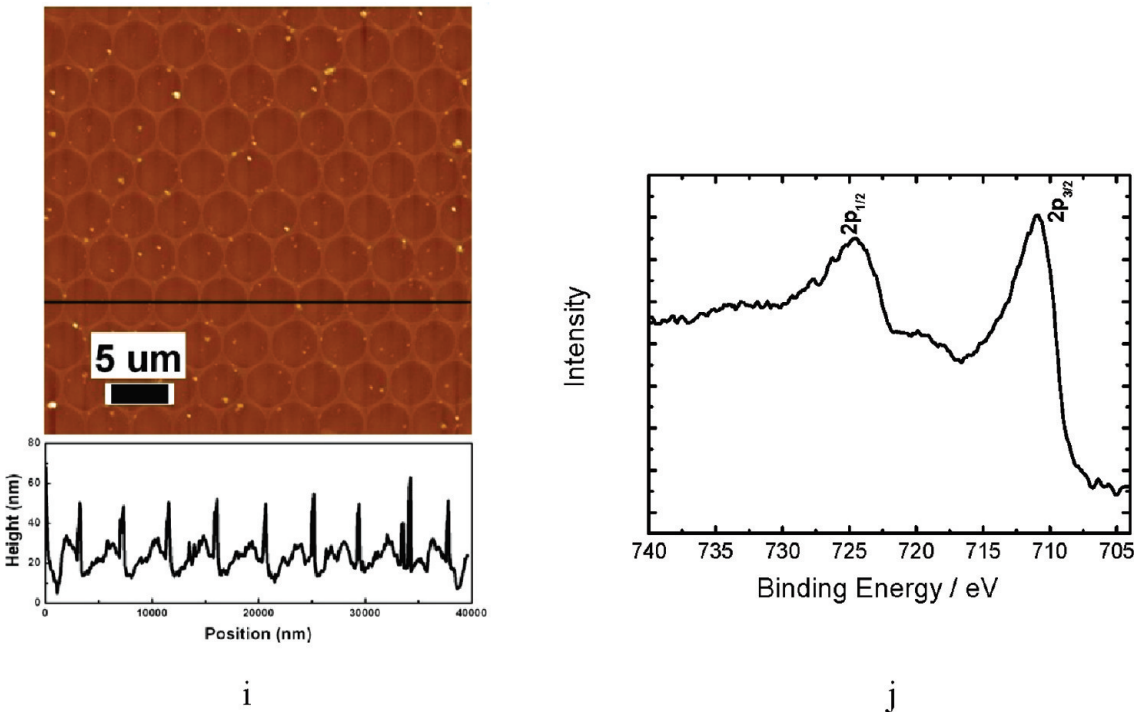

Figure 2. (a) Photograph of sunlight diffraction obtained from a honeycomb structured PSPAA/ferrocene hybrid film on Si substrate. (b) SEM and (c) topographic images of the honeycomb structured PSPAA/ferrocene hybrid film. The FFT in the inset shows the very regular character of the main structures. (d) Cross-section view of honeycomb structured PSPAA/ferrocene hybrid film. (e) SEM image of honeycomb structured PSPAA/ferrocene hybrid film after 4 h UV irradiation. f) Cross-section view of honeycomb structured PSPAA/ferrocene hybrid film after 4 h UV irradiation. (g) SEM image of cross-linked PSPAA/ferrocene hybrid film after heating at 750 °C for 10 min. (h) SEM image of cross-linked PSPAA/ferrocene hybrid film pyrolyzed at 450 °C for 5 h. (i) Cross-section line scan profile of cross-linked PSPAA/ferrocene hybrid film pyrolyzed at 450 °C for 5 h. (j) XPS core level scan of Fe after pyrolysis.

The synthesis of organic/inorganic hybrid materials using organic polymers as structure directing agents or templates is an area of rapid growth.[12] Block copolymers are super structure-directing agents for solution, bulk, and surface. However, upon heating up to 100 °C (the glass transition temperature, T_g, of the PS matrix), the as-prepared microporous hybrid film began to melt then collapsed and totally disappeared at 130 °C. The poor thermal stability causes the structure-directing action of the polymer matrix invalid in the following CVD process. No special CNT arrays were found on substrate. Cross-linkage should be an efficient method targeting the stable film structure against solvents and heat annealing.[13] To improve the thermal stability of the polymer matrix, the honeycomb structured hybrid film was exposed in deep UV light. The UV cross-linking mechanisms of PS and PAA have been explained in detail.[14] This technique has been further developed to fabricate nanoporous functional polymeric films by selectively cross-linking PS matrix and degrading polymethylmethacrylate (PMMA) minority in PSPMMA diblock copolymer.[15]

Recently, we also reported the use of this simple method to improve thermal stability and surface wettability of microporous polymer films simultaneously.[10] Compared with chemical cross-linking, photochemical cross-linking process is operated at room temperature and easy to control, so the process not only effectively cross-links the polymer matrix but also facilitates the preservation of ordered structures. Similar nacre colors were seen on silicon wafer (see the Supporting Information, Figure S1), on which an ordered PSPAA/ferrocene hybrid film was exposed in UV light for 4 h. The top-view and cross-section SEM views are shown in images e and f in Figure 2, respectively. It is evident that both the honeycomb patterns and spatial structures in the hybrid film are highly maintained without collapse. After UV irradiation, the thermal stability of cross-linked polymer matrix was significantly improved because of the prohibited unzipping and depropogation processes.[16] Because the photochemical cross-linking occurs mostly on film surface, the hybrid film after UV irradiation could survive at 750 °C for 10 min (the same as the CVD process)

(12) (a) Karthaus, O.; Cieren, X.; Maruyama, N.; Shimomura, M. *Mater. Sci. Eng., C* **1999**, *10*, 103. (b) Zhang, K.; Zhang, L. W.; Chen, Y. M. *Macromol. Rapid Commun.* **2007**, *28*, 2024. (c) Englert, B. C.; Scholz, S.; Leech, P. J.; Srinivasarao, M.; Bunz, U. H. F. *Chem.—Eur. J.* **2005**, *11*, 995.

(13) (a) Yabu, H.; Kojima, M.; Tsubouchi, M.; Onoue, S.; Sugitani, M.; Shimomura, M. *Colloids Surf., A* **2006**, *284−285*, 254. (b) Ergodan, B.; Song, L.; Wilson, J. N.; Park, J. O.; Srinivasarao, M.; Bunz, U. H. F. *J. Am. Chem. Soc.* **2004**, *126*, 3678. (c) Karthaus, O.; Hashimoto, Y.; Kon, K.; Tsuriga, Y. *Macromol. Rapid Commun.* **2007**, *28*, 962.

(14) (a) Rãnby, B.; Rabek, J. F. *Photodegradation, Photooxidation and Photostabilization of Polymers*; Wiley: New York, 1975. (b) Melo, M. J.; Bracci, S.; Camaiti, M.; Chiantore, O.; Piacenti, F. *Polym. Degrad. Stab.* **1999**, *66*, 23.

(15) (a) Thurn-Albrecht, T.; Schotter, J.; Kastle, C. A.; Emley, N.; Shibauchi, T.; Krusin-Elbaum, L.; Guarini, K.; Black, C. T.; Tuominen, M. T.; Russell, T. P. *Science* **2000**, *290*, 2126. (b) Thurn-Albrecht, T.; Steiner, R.; DeRouchey, J.; Stafford, C. M.; Huang, E.; Bal, M.; Tuominen, M.; Hawker, C. J.; Russell, T. P. *Adv. Mater.* **2000**, *12*, 1138. (c) Yang, S. Y.; Ryu, I.; Kim, H. Y.; Kim, J. K.; Jang, S. K.; Russell, T. P. *Adv. Mater.* **2006**, *18*, 709.

(16) Levchik, G. F.; Si, K.; Levchik, S. V.; Camino, G.; Wilkie, C. A. *Polym. Degrad. Stab.* **1999**, *65*, 395.

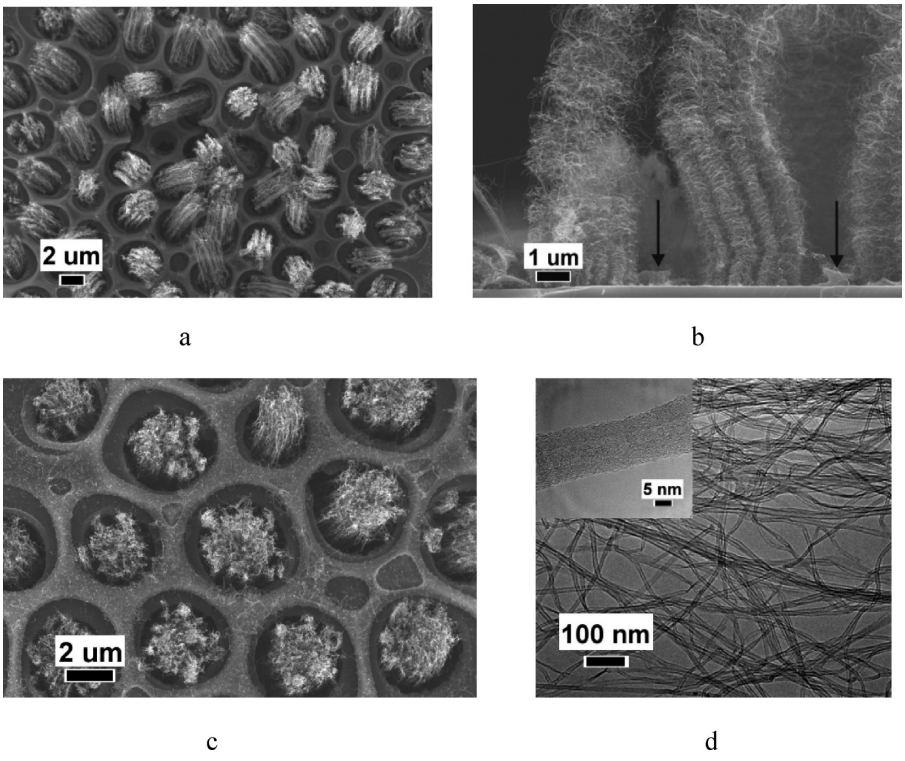

Figure 3. SEM images of the patterned CNTs with circular pillars in the centers of honeycomb patterns, viewed from (a) top and (b) side, respectively; (c) SEM image of the high quality of the aligned CNT bundles, just like one end of a serial port. (d) HRTEM images of the patterned CNTs in a; the inset shows one multiwalled carbon nanotube.

with well-preserved surface features, whereas the film thickness shrank significantly because of the collapse of uncross-linked polymer stratum (Figure 2g). Additionally, the cross-linked polymer matrix could act as structure-directing agent to form regular micropatterns by a programmed pyrolysis process as described in the Experimental Section. SEM observation (Figure 2h) reveals that the walls of the obtained micropatterns become thinner and sharper, suggesting that much material was burned off (an SEM top view in large scan is demonstrated in the Supporting Information, Figure S2). The cross-section line scan profile (Figure 2i) indicates the hole depth was reduced to 50 nm. TG analysis indicates that 96% weight loss was achieved (see the Supporting Information, Figure S3). The core scan of Fe (Figure 2j) definitely shows that the incorporated ferrocene has been partially oxidized to Fe_2O_3. In other words, pyrolysis decomposes the polymer matrix and converts the incorporated ferrocene into the skeleton of inorganic micropatterns simultaneously. The formed micropatterns have the identical spacing with that of the micropores on the as-prepared film surface, indicative of the in situ formation of inorganic patterns on the honeycomb structures. It should be noted that many other microstructured ceramic films, having potential use in photonic crystals, magnetic and electronic materials, could be prepared by the similar methodology simply by choosing different functional precursors without the need of particular chemical reaction and time-consuming synthesis.[12c] The cross-linked polymer matrix and the ferrous inorganic micropatterns are used as the templates to grow the both ends of a pair of serial-port-shaped aligned CNT bundles as discussed below.

In particular, CVD provides an effective technique of growing CNTs from controlled surface sites by catalyst patterning on a desired substrate[17] for specific applications, e.g., for field-emission displays, a specific architecture of a nanotube device or probe tips of scanning probe microscopes.[18−20] rein, patterned CNTs were synthesized with constant flow rate of 500/200/78 for $Ar/H_2/C_2H_2$. The growth temperature was 750 °C and the growth time was about 10 min. To avoid undesired vaporization of ferrocene during the ramping step, we kept the Si wafer with cross-linked hybrid film (pulling out the wafer to prevent ferrocene from the heating zone) at the cool end of the furnace before the furnace was heated to the working temperature. After the furnace reached the preset temperature, the substrate was pushed back to keep the substrate at the center of the furnace, and then C_2H_2 was carried into the reactor by a gas mixture of Ar and H_2 through a bubbler. Starting from cross-linked polymer matrix template (Figure 2g), isolated CNT bundles were formed, as shown in Figure 3a. A close examination reveals that CNT bundles developed from the cavities exclusively and were isolated by the walls of the remained honeycomb

(17) (a) Ren, Z. F.; Huang, Z. P.; Wang, D. Z.; Wen, J. G.; Xu, J. W.; Wang, J. H.; Calvet, L. E.; Chen, J.; Klemic, J. F.; Reed, M. A. *Appl. Phys. Lett*. **1999**, *75*, 1086. (b) Bonard, J. M.; Kind, H.; Stöckli, T.; Nilsson, L. O. *Solid-State Electron*. **2001**, *45*, 893.
(18) Choi, W. B.; Chung, D. S.; Kang, J. H.; Kim, H. Y.; Jin, Y. W.; Han, I. T.; Lee, Y. H.; Jung, J. E.; Lee, N. S.; Park, G. S.; Kim, J. M. *Appl. Phys. Lett*. **1999**, *75*, 3129.
(19) Dai, H. J.; Kong, J.; Zhou, C. W.; Franklin, N.; Tombler, T.; Cassell, A.; Fan, S. S.; Chapline, M. *J. Phys. Chem. B* **1999**, *103*, 11246.
(20) Hafner, J. H.; Cheung, C. L.; Lieber, C. M. *J. Am. Chem. Soc*. **1999**, *121*, 9750.

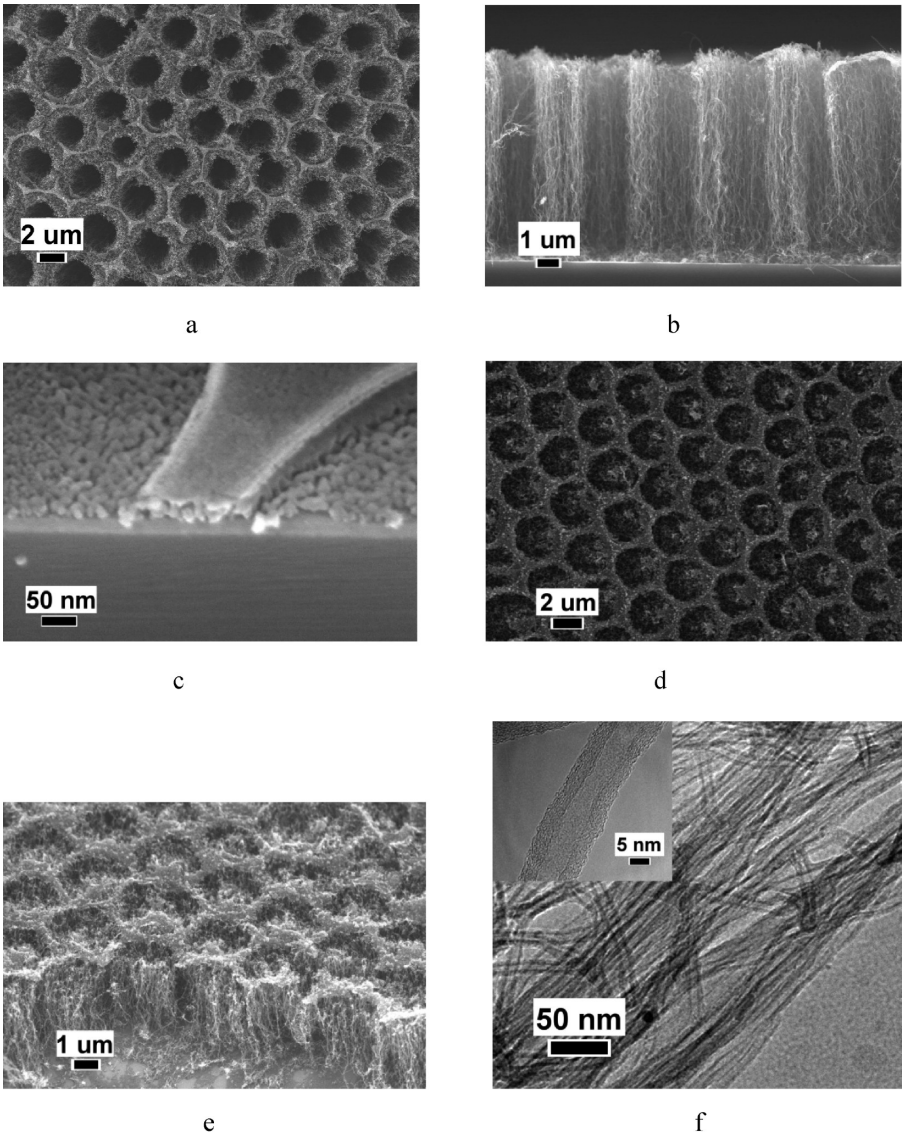

Figure 4. SEM images of the patterned CNTs with a honeycomb structure, viewed from (a) top and (b) side, respectively. (c) Cross-section SEM view of ferrous inorganic micropatterns. SEM images of dense CNT bundles grown on Si wafer coated by SiO_2, (d) top view; (e) cross-section view. (f) HRTEM image of the patterned CNTs in Figure 4a, the inset showed one multiwalled carbon nanotube.

structures, as pointed by the arrows (Figure 3b). The selective growth of isolated CNT bundles from the cavities is attributed to the selectively interfacial aggregation of ferrocene to the walls of the cavities, a so-called Pickering-emulsion effect,[21] whereas in the past few years, people have reconsidered the possibilities of using fluid interface to control the assembly of nanoparticles.[22] In a typical BF formation process, water droplets floating on the surface of the solution are arranged into highly ordered arrays. Hence it introduces patterned liquid/liquid interfaces that can be utilized to control the assembly and alignment of ferrocene particles with interfacial activities. Before the polymer film becomes too viscous, the ferrocene particles can aggregate to the interface and form a uniform layer. As the concentration of the polymer/ferrocene mixture increases with solvent evaporation, the film passes through the glass transition of the polymer at room temperature and locks the droplets and the ferrocene particles into place. On evaporation of the water, spherical cavities remain where the walls are decorated with the ferrocene particles.[23] In the following UV irradiation, the ferrocene particles either on the walls of cavities or embedded in the hybrid film were locked by the cross-linked polymer matrix. Upon H_2 treatment, ferrocene particles exposed on the cavity walls was reduced and became activated, which initiated the growth of CNTs in the cavities. However, the ferrocene particles embedded in the hybrid film shielded from cross-linked polymer skin were isolated from H_2 and acetylene gas (carbon source), which cause the selective growth. It is found that the bottoms of the CNT

(21) Pickering, S. U. *J. Chem. Soc.* **1907**, *91*, 2001.
(22) (a) Duan, H.; Wang, D.; Kurth, D. G.; Möhwald, H. *Angew. Chem., Int. Ed.* **2004**, *43*, 5639. (b) Wang, J.; Wang, D.; Sobal, N. S.; Giersig, M.; Jiang, M.; Möhwald, H. *Angew. Chem., Int. Ed.* **2006**, *45*, 7963.
(23) (a) Boker, A.; Lin, Y.; Chiapperini, K.; Horowitz, R.; Thompson, M.; Carreon, V.; Xu, T.; Abetz, C.; Skaff, H.; Dinsmore, A. D.; Emrick, T.; Russell, T. P. *Nat. Mater.* **2004**, *3*, 302. (b) Sun, W.; Ji, J.; Shen, J. *Langmuir* **2008**, *24*, 11338.

bundles are confined in the trenches and vertically fixed onto the substrate. Figure 3c shows the high quality of the aligned CNT bundles, just like one end of a serial port. Beyond the height of the cavities, the bundles begin to tilt and aggregate with the adjacent bundles because of the gravity (Figure 3a).[24] The thickness of the remained polymer matrix as pointed by the arrow is close to 500 nm. HRTEM image definitely shows that the formed CNTs were multiwalled tubes having an average diameter of 15 nm (Figure 3d).

Templating from ordered inorganic ferrous micropattens, honeycomb-like skeleton of dense CNT bundles (another end of a serial port) were formed after CVD process, as shown in Figure 4a. The spacing of the skeleton is identical with that of the inorganic micropatterns, indicative of the in situ formation of inorganic patterns on the honeycomb structures. Cross-sectional view demonstrates that the aligned CNTs are perpendicular to substrate without collapse (Figure 4b), because the supporting force among the continuous CNT bundles counteracted the effect of gravity. The well-aligned CNT bundles have a uniform length of 8 μm and can be controlled by changing the time of CVD process. The change of CNT arrays from isolated bundles to continuous CNT honeycomb structures is explained as the follows. During the pyrolysis, polymer matrix was graduatelly decomposed and the cavity bottoms sunk down on substrate, a chemical reaction occurs between the silicon and ferrocene dominated by diffusion of ferrocene through the silicon wafer at high temperature.[25] These result in a complete change in the chemical nature of an active ferrocene catalyst to stable compounds such as iron silicide ($FeSi_2$) and iron silicate (Fe_2SiO_4), which are known for their noncatalytic activity for carbon nanotube growth.[26] Usually, there exists a 2 nm thick native oxide layer on the commercially available Si wafer (determined by ellipsometer in our lab). It cannot prevent Fe from ferrocene diffuses through SiO_2 layers and react with the Si substrate, leading to the formation of $FeSi_2$ and $FeSiO_4$.[27] On the other hand, the ferrocene particles embedded in the polymer matrix, especially on the hexagonal edges, were oxidized and exposed to surface because most of the polymer composition has been burned off during the pyrolysis. AFM height image indicates that the height difference between the edges and bottoms in the inorganic micropatterns is 50 nm (Figure 2i), which is thick enough to isolate the ferrous composition from the Si substrate. The cross-section SEM view (Figure 4c) definitely reveals that the Si wafer is covered by a thin layer of surface-featured ferrous inorganic film. Although partial ferrocene was oxidized into Fe_2O_3, they still can be reduced and effectively catalyze the growth of highly dense carbon nanotubes into the approximately hexagonal shape. To further confirm this explanation, we employed Si wafers coated by SiO_2 as substrates in order to preclude the chemical reactions between ferrocene and Si wafers. The thickness of the coated SiO_2 layer is 400 nm, much thicker than the critical thickness of 5 nm as discussed in ref 27. After the same photochemical cross-linking, pyrolysis, and CVD process, dense and vertical CNT bundles were formed on coated substrate (Figure 4d,e). The formed CNTs are multiwalled tubes having an average diameter of 15 nm, as confirmed by high-resolution transmission electron microscopy and shown in Figure 4f.

In summary, we have synthesized a pair of patterned carbon nanotubes with the shape of serial port by CVD starting from different breath figure templates, cross-linked polymer matrix, and ferrous inorganic micropatterns. The growth mechanism of the isolated CNT bundles is attributed to the selectively interfacial aggregation of the ferrocene to the walls of the cavities, a so-called Pickering-emulsion effect, whereas the honeycomblike skeleton of the dense CNT arrays develop from the catalytically functionalized hexagonal edges. This synthesis strategy exemplifies a new possibility for making use of CNTs to fabricate functional carbons with unique geometry or specific properties in a controllable way, which may also shed some light on further understanding, both experimentally and theoretically, of the self-assembly of CNTs. In addition, the fabrication of patterned graphene by means of the static BF technique is currently under investigation.

Experimental Section

Materials. Ferrocene and carbon disulfide (CS_2) were purchased from Shanghai Chemical Reagent Plant. All the chemical reagents were used without further purification. Silicon wafers were used as-received. The preparation of PSPAA diblock copolymer was synthesized via atom-transfer radical polymerization in a similar procedure as reported in ref 28.

The relative molecular weights of PS and PAA blocks were 9000 and 2500 g mol^{-1}, respectively. The molecular weight distribution (M_w/M_n) of such diblock copolymer was 1.07. The relative molecular weights and M_w/M_n were measured by a Waters gel permeation chromatography (GPC) system equipped with a Waters 1515 Isocratic HPLC pump, a Waters 2414 refractive index detector (RI), a Waters 2487 dual λ absorbance detector (UV) and a set of Waters Styragel columns (HR3, HR4 and HR5, 7.8 $\times$ 300 mm). GPC measurements were carried out at 35 °C using tetrahydrofuran (THF) as an eluent with a flow rate of 1.0 mL/min. The system was calibrated with polystyrene standards.

Preparation of Honeycomb Structured Hybrid Films. The static breath-figure process was operated in a 25 mL straight-mouth glass bottle with a cap. A saturated relative humidity in the vessel was achieved by adding 2 mL of distilled water into the bottle beforehand. A piece of substrate was adhered onto the top of a plastic stand with double-sided tape and placed into the glass vessel. The substrate was 1 cm higher than the liquid level.

Polymer and ferrocene were mixed with a fixed weight ratio (5/1, w/w) and dissolved in CS_2. The solution concentration was

(24) Wu, J.; Huang, Q. W.; Ma, Y. F.; Huang, Y.; Liu, Z. F.; Yang, X. Y.; Chen, Y. S.; Chen, D. P. *Colloids Surf., A* **2008**, *313*, 13.
(25) Jung, Y. J.; Wei, B. Q.; Vajtai, R.; Ajayan, P. M. *Nano Lett.* **2003**, *3*, 561.
(26) De los Arcos, T.; Vonau, F.; Garnier, M. G.; Thommen, V.; Boyen, H. G.; Oelhafen, P.; Duggelin, M.; Mathis, D.; Guggenheim, R. *Appl. Phys. Lett.* **2002**, *80*, 2383.
(27) Cao, A. Y.; Ajayan, P. M.; Ramanatha, G.; Baskaran, R.; Turner, K. *Appl. Phys. Lett.* **2004**, *84*, 109.
(28) Kang, Y. J.; Taton, T. A. *Angew. Chem., Int. Ed.* **2005**, *44*, 409.

15 mg mL^{-1}. The honeycomb film was prepared by casting 100 μL of solution onto the substrate with a microsyringe. With organic solvent volatilization, the transparent solution became turbid. The film was taken out for microscope observation after complete solvent evaporation. All the experiments were carried out at room temperature unless stated otherwise.

Photochemical Cross-Linking and Pyrolyzing. The photochemical cross-linking was performed at 30 °C in a UVO cleaner ZWLH-5 (Tianjin, China) at the presence of air, by exposing the polymer thin films into UV light. The cleaner generated UV emission at a wavelength of 254 nm and power of 500 W. The distance between the UV source and the film surface was 10 cm. After 4 h UV exposure, the cross-linked film was heated to 450 °C within 2 h and held for another 5 h under air atmosphere. During the pyrolysis, ferrocene turned into oxide and replaced the polymer skeleton eventually.

Preparation of Carbon Nanotube Arrays. Aligned CNT arrays were synthesized by thermal chemical vapor deposition (CVD) in a 40 mm diameter quartz tube furnace. The tube furnace was preheated to 750 °C and then the templates were inserted into the chamber. An Ar/H_2 gas mixture was used as the buffer gas and pure acetylene served as the carbon source. In the growth process, a constant flow rate of 500/200/78 sccm (standard-state cubic centimeter per minute) for $Ar/H_2/C_2H_2$ was used. The growing time was 10 min.

Characterization and Apparatus. The morphology and structure of patterned carbon nanotubes were characterized by a Hitachi S4800 scanning electron microscope (SEM). A 10 KeV electron beam was used for the observation with a working distance of 8 mm in order to obtain secondary electron images. Atomic force microscopy (AFM) measurements were carried out in the tapping mode with a Seiko Instruments SPA400. We used silicon tips with a spring constant of 20 N/m. X-ray photoelectron spectroscopy (XPS) spectra were acquired with a PHI Quantum 2000 spectrometer using monochromated X-rays from an $Al_{K\alpha}$ source with a takeoff angle of 45° from the surface plane. The atomic fractions of carbon and oxygen were computed using the attenuation factors provided by the supplier and the sum of these atomic fractions was normalized to unity. Thermogravimetric (TG) analysis was taken on a Netzsch STA 409 EP Thermal Analyzer. The sample was heated from 25 to 450 °C at a rate of 5 °C/min and held for 5 h under air. The morphology and structure of the carbon nanotubes were characterized by high-resolution transmission electron microscopy (TEM, TECNAI F-30) with an acceleration voltage of 300 kV. The TEM specimens were prepared by dispersing the CNTs in ethanol. A drop of the suspension was deposited on a carbon-film-coated copper grid.

Acknowledgment. L.L. gratefully acknowledges the National Natural Science Foundation of China (50703032 and 20974089), the Natural Science Foundation of Fujian Province (2009J06029), and the Program for New Century Excellent Talents of Ministry of Education of China.

Note Added after ASAP Publication. Parts i and j of Figure 2 were missing in the version published ASAP February 16, 2010; the corrected version was published ASAP March 18, 2010.

Supporting Information Available: Three additional figures (PDF). This material is available free of charge via the Internet at http://pubs.acs.org.